Phys. Status Solidi A **211**, No. 1, 226–230 (2014) / **DOI** 10.1002/pssa.201330203

physica status solidi a
www.pss-a.com
applications and materials science

Effects of Nb_2O_5 additive on the piezoelectric and dielectric properties of PHT-PMN ternary ceramics near the morphotropic phase boundary

Dawei Wang*,[1], Jinglin Li[2], Maosheng Cao[3], and Shujun Zhang,[4]**

[1] College of Mechanical and Electrical Engineering, North China University of Technology, Beijing 100144, P. R. China
[2] Changchun Institute of Optics, Fine Mechanics and Physics, Chinese Academy of Sciences, Changchun 130033, P. R. China
[3] School of Materials Science and Engineering, Beijing Institute of Technology, Beijing 100081, P. R. China
[4] Materials Research Institute, Pennsylvania State University, University Park, PA 16802, USA

Received 6 August 2013, revised 18 September 2013, accepted 4 October 2013
Published online 8 November 2013

Keywords dielectric properties, ferroelectric properties, $PbHfO_3$-$PbTiO_3$-$Pb(Mg_{1/3}Nb_{2/3})O_3$, piezoelectric properties

* Corresponding author: e-mail wangdawei102@gmail.com, Phone/Fax: +86 010 88802632
** e-mail soz1@psu.edu, Phone: 814 863-2639, Fax: 814 865-2326

Recently, a new family of piezoelectric perovskite materials, $PbHfO_3$-$PbTiO_3$-$Pb(Mg_{1/3}Nb_{2/3})O_3$ (PHT-PMN) ternary system was developed, possessing good piezoelectric properties and high Curie temperature near the morphotropic phase boundary (MPB). Nb_2O_5, as a donor dopant in the perovskite piezoelectric systems has been used to improve the dielectric and piezoelectric properties. In this work, the effect of Nb_2O_5 addition in the PHT-PMN ternary system was reported. It was found that Nb doping led to the change of phase structure for the PHT-PMN system. With the addition of Nb_2O_5 content, the ferroelectric polarization was reduced, while the electric-field-induced strain and hysteresis were enhanced significantly. In particular, the 0.2 wt% Nb_2O_5-doped PHT-PMN exhibited the optimum piezoelectric and electromechanical properties, with d_{33} and k_p being on the order of 670 pC N^{-1} and of 71%, respectively.

1 Introduction Perovskite materials have been extensively studied for actuators, sensors, and transducers applications, because of their high dielectric and piezoelectric properties, particularly for the $PbZrO_3$-$PbTiO_3$ (PZT) solid solution system [1, 2]. The highest piezoelectric response is found for compositions in the vicinity of the morphotropic phase boundary (MPB), separating the rhombohedral and tetragonal ferroelectric phases, which is an abrupt structural change with composition and nearly temperature independent [3]. Furthermore, numerous studies on PZT-based ternary solid solutions, such as $Pb(Mg_{1/3}Nb_{2/3})O_3$-$PbZrO_3$-$PbTiO_3$ (PMN-PZT) [4, 5], $Pb(Ni_{1/3}Nb_{2/3})O_3$-$PbZrO_3$-$PbTiO_3$ (PNN-PZT) [6, 7], $Pb(Mg_{1/3}Ta_{2/3})O_3$-$PbZrO_3$-$PbTiO_3$ (PMT-PZT) [8, 9], and $Pb(Yb_{1/2}Nb_{1/2})O_3$-$PbZrO_3$-$PbTiO_3$ (PYN-PZT) [10, 11] have been carried out and their MPB compositions were reported to exhibit promising dielectric and piezoelectric properties.

Analogous to PZT, $PbHfO_3$-$PbTiO_3$ (PHT) solid solution with MPB composition was reported to possess dielectric and piezoelectric properties comparable to PZT [12, 13]. To date, however, limited studies have been carried out on the PHT-$Pb(A_1,A_2)O_3$ based ternary systems, which are expected to exhibit good dielectric/piezoelectric properties with high Curie temperature. Recently, $PbHfO_3$-$PbTiO_3$-$Pb(Mg_{1/3}Nb_{2/3})O_3$ (PHT-PMN) was systematically studied, exhibiting higher T_C and improved piezoelectric and electromechanical properties when compared to those of commercial PZT5H [14, 15], demonstrating a promising candidate for transducer applications at elevated temperature.

It is well known that the structure and electrical properties of piezoelectric ceramics can be tailored to meet different requirements by introducing various additives [16–19]. Nb_2O_5 is one of the most used additives to enhance the dielectric and piezoelectric properties of PZT [20–26]. Garcia et al. [21] revealed that Nb^{5+} as a donor impurity considerably increased the mobility of domain walls and also the dielectric and piezoelectric non-linear response. Thakur et al. [23] reported that the maximum dielectric permittivity and remnant polarization increased with Nb^{5+} addition. In addition, the introduction of Nb_2O_5 in PZT-based system could improve the densification of ceramics and strongly reduce grain size, leading to the improvement of both piezoelectric and mechanical properties [24–26]. In this work, Nb_2O_5 was introduced into PHT-PMN ceramics in order to improve the piezoelectric and electromechanical properties. The effects of Nb_2O_5 additive on the phase structure, dielectric, piezoelectric properties, and electric-field-induced polarization and strain of the PHT-PMN ceramics were studied.

2 Experimental PHT-PMN ternary ceramics with compositions of $0.8Pb(Hf_{0.446}Ti_{0.554})O_3$-$0.2Pb(Mg_{1/3}Nb_{2/3})O_3 + xNb_2O_5$ (0.8PHT-0.2PMN + $x$$Nb_2O_5$, $x = 0$, 0.2, 0.5, 0.8, and 1.0 wt%) were prepared using the two-step precursor method. The detailed preparation procedure of PHT-PMN ternary ceramic powders can be found in previous reports [14, 15]. Nb_2O_5 (99.9%) with different doped levels were added and subsequently vibratory milled in alcohol for 12 h. The powders were then granulated and pressed into pellets with 12 mm in diameter. Following binder burn-out at 550 °C, the pellets were sintered in a sealed crucible at 1200 °C, where $PbZrO_3$ was used as lead source to minimize PbO evaporation.

The phase structure was determined using X-ray powder diffraction (XRD). Silver paste was printed to form electrodes on both sides of the disk samples and then fired at 700 °C. Poling was carried out in silicon oil at 120 °C for 10 min with an electric field of 30 kV cm^{-1}. Dielectric measurements were carried out using a multi-frequency precision LCRF meter (HP 4184A). The piezoelectric coefficients were measured using a Berlincourt d_{33} meter. Polarization hysteresis and strain-electric field behavior were determined using a modified Sawyer-Tower circuit driven by a lock-in amplifier (Model SR830). The planar electromechanical coupling factor k_p was determined from the resonance and antiresonance frequencies, which were measured using an Impedance/Gain-phase analyzer (HP 4194A, Hewlett-Packard, Palo Alto, CA, USA) according to IEEE standards [27, 28].

3 Results and discussion XRD patterns of Nb_2O_5-modified 0.8PHT-0.2PMN with various Nb_2O_5 contents are shown in Fig. 1. All studied samples were found to be pure perovskite and there was no evidence of a second phase, indicating that Nb ions diffused into the crystal lattice of 0.8PHT-0.2PMN and formed a stable solid-solution. Furthermore, the crystal structure of the samples was varied clearly by the addition of Nb_2O_5, as revealed by changing of the split (200) and (002) peaks, as presented in Fig. 1(b). It should be noted that the studied compositions were located at the MPB region, being indicated by the broadening of (200) peaks. The two slightly split peaks at about 45° observed in the diffractogram of 0.8PHT-0.2PMN progressively merged

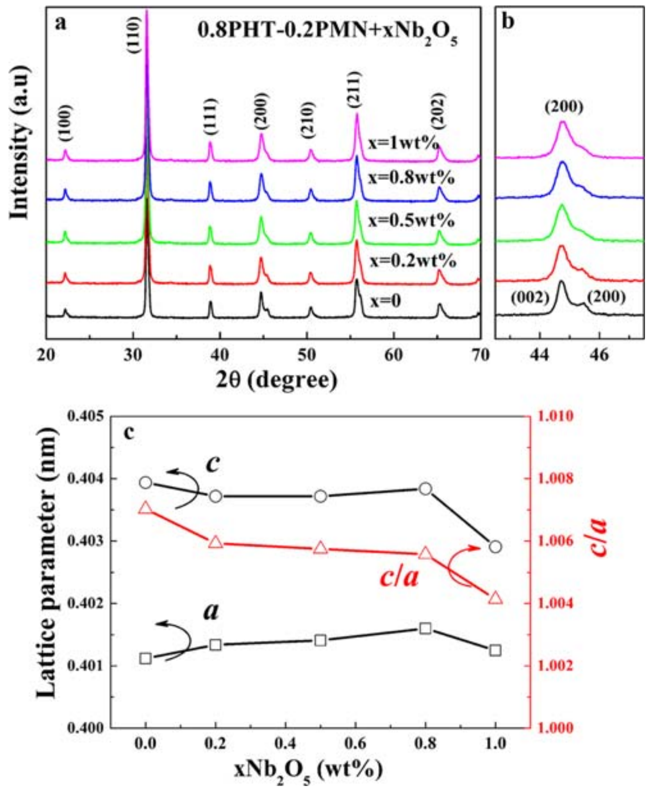

Figure 1 (a) XRD patterns of Nb_2O_5 doped 0.8PHT-0.2PMN; (b) corresponding expanded XRD patterns in the range of 2θ from 42° to 48°; and (c) the corresponding lattice parameters a, c, and tetragonality c/a of 0.8PHT-0.2PMN as a function of Nb_2O_5 content.

with increasing Nb_2O_5 content. This indicates the transformation of the perovskite lattice from tetragonal to rhombohedral, confirmed by the decrease of calculated tetragonality (c/a), the corresponding lattice parameters a, c, and c/a were given in Fig. 1(c). Earlier studies have reported that Nb^{5+} ions could enter the B-sites of PZT lattice and substitute Zr^{4+}/Ti^{4+} ions (note that the ionic radii and the charges of these ions are similar) [23, 25]. Analogous to the PZT-based system, in this work, the phase transformation in PHT-based solid-solution is deemed to be related to the substitution of Nb^{5+} ions for the B-site ions in the perovskite structure. It was explained that the stronger Nb–O bond leads to the movement of O^{2-} toward Nb^{5+}, resulting in the motion of Pb^{2+} toward Nb^{5+} simultaneously, due to the restriction of Pb–O bond. As a result, the perovskite structure of PHT-PMN will contract and the symmetry axis gradually changes from the direction of <001> to <111>, leading to the crystal structure transforming from tetragonal to rhombohedral with increasing Nb_2O_5 content [23].

The temperature dependence of dielectric permittivity ε_r and loss tanδ for Nb_2O_5-modified 0.8PHT-0.2PMN is given in Fig. 2. It was found that with increasing Nb_2O_5 content, the Curie temperature T_C decreased from 276 to 256 °C gradually, as listed in Table 1, which is consistent with previous reports [22–24]. Furthermore, the broadened

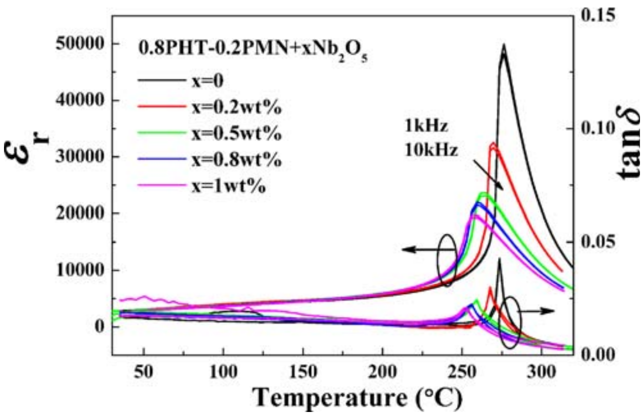

Figure 2 Temperature dependence of dielectric permittivity ε_r and loss tanδ for Nb_2O_5 doped 0.8PHT-0.2PMN.

dielectric peaks and dispersive dielectric behavior with respect to frequency were observed for Nb-doped compositions, especially for the compositions with doped level higher than 0.2 wt%, indicative of diffused phase transition behavior, as shown in Fig. 2. The incorporation of niobium on the B-site creates vacancies in the A-site of the perovskite structure. It is believed to break the long-range interaction between ferroelectrically active oxygens in BO_6 octahedron, which affects the ferroelectric properties of the system [29]. Then, for a higher Nb content, a lower thermal energy will be necessary to provide a ferroelectric–paraelectric transition, decreasing T_C [23]. With further increasing doped level, the excess of Nb_2O_5 will go into the grain boundary, which smear the dielectric peak [22, 23].

The bipolar polarization hysteresis loops of Nb_2O_5-modified 0.8PHT-0.2PMN are shown in Fig. 3a, from which the remnant polarization P_r and coercive field E_C as a function of Nb_2O_5 content can be obtained, as given in Fig. 3b. It was found that with increasing Nb_2O_5 content, P_r decreased monotonously from 41.5 to 35 $\mu C\,cm^{-2}$, while E_C increased from 8.8 to 10.6 $kV\,cm^{-1}$, indicating that the domain switching becomes harder with higher Nb_2O_5 doped level. Due to the coexistence of ferroelectric rhombohedral and tetragonal phases in the MPB region, the highest P_r value of 41.5 $\mu C\,cm^{-2}$ in PHT-PMN is expected owing to the summation of the possible crystallographic orientations,

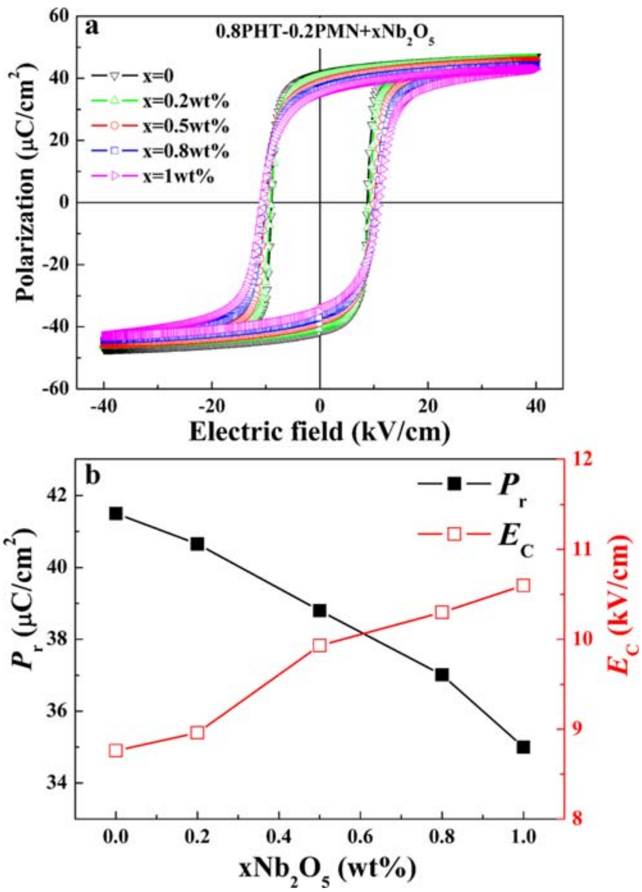

Figure 3 (a) Bipolar polarization hysteresis loops and (b) the remnant polarization P_r and coercive field E_C as a function of Nb_2O_5 content.

with eight <111> spontaneous polarization directions in a rhombohedral phase and six <001> directions in a tetragonal phase [15, 30]. However, with increasing Nb_2O_5 content, the crystal structure gradually transformed to the rhombohedral dominated phase, leading to the deterioration of polarizability arising from reduced coupling between ferroelectric rhombohedral and tetragonal phases. On the other hand, the decreased grain size due to the Nb dopant will increase the coercive field [26].

Table 1 Piezoelectric, dielectric and ferroelectric properties of Nb_2O_5-doped 0.8PHT-0.2PMN ternary ceramics (*Ref. [36]; d_{33}, piezoelectric coefficient; k_p, planar electromechanical coupling; ε_r, dielectric permittivity; tanδ, dielectric loss; T_C, Curie temperature; P_r, remnant polarization; E_C, coercive field; d^*_{33}, high field piezoelectric strain coefficient).

Nb_2O_5 content	d_{33} ($pC\,N^{-1}$)	k_p (%)	ε_r @1 kHz	tanδ (%)	T_C (°C)	P_r ($\mu C\,cm^{-2}$)	E_C ($kV\,cm^{-1}$)	d^*_{33} ($pm\,V^{-1}$)
0	660	70	2790	1.5	276	41.5	8.8	560
0.2 wt%	670	71	2730	1.6	269	40.7	9.0	580
0.5 wt%	610	69	2700	1.7	263	38.8	9.9	670
0.8 wt%	590	67	2700	1.8	259	37.0	10.3	680
1 wt%	540	65	2700	1.8	256	35.0	10.6	700
PZT5H	593	65	3400	2	193	33	7.5	720

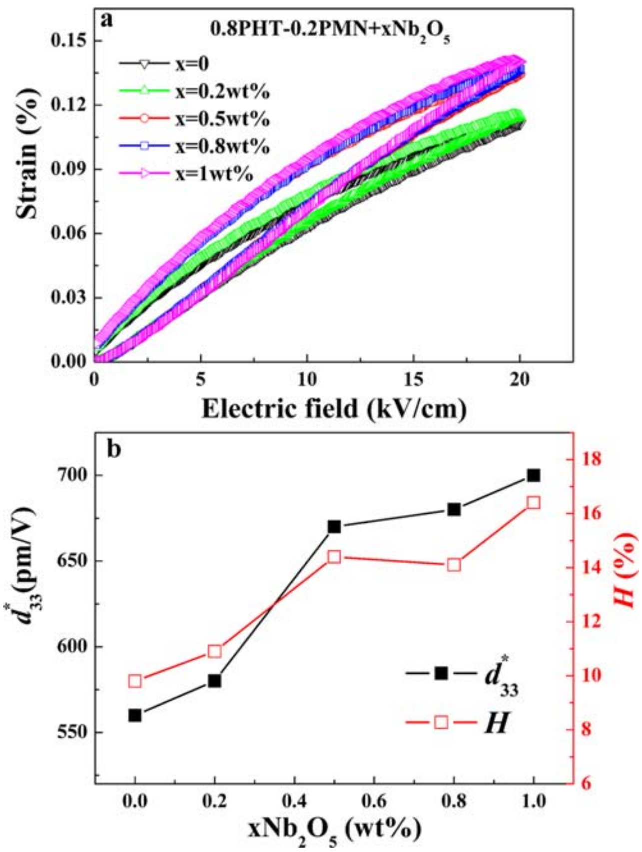

Figure 4 (a) The unipolar strain–electric field curves for Nb_2O_5 doped 0.8PHT-0.2PMN ceramics and (b) the high-field piezoelectric strain coefficient d^*_{33} and strain hysteresis H as a function of Nb_2O_5 content.

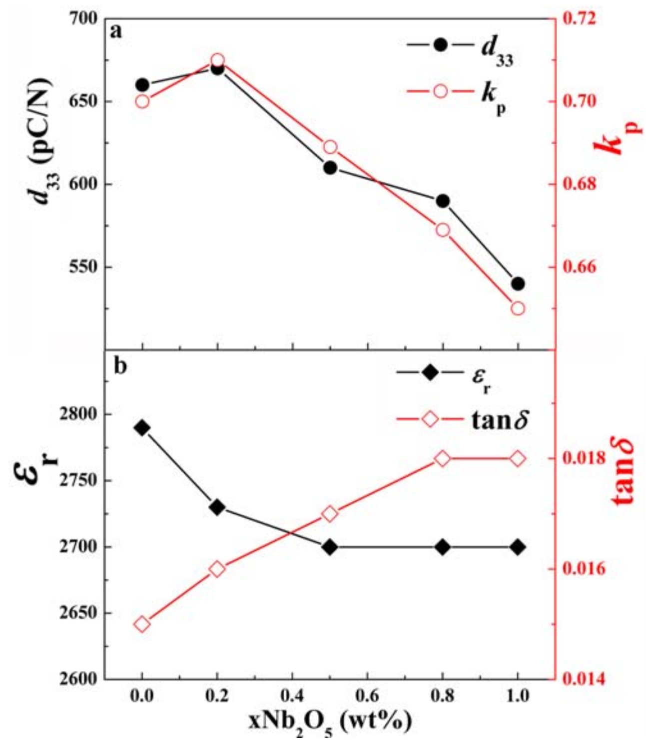

Figure 5 (a) Piezoelectric coefficient d_{33} and planar electromechanical coupling k_p, (b) dielectric permittivity ε_r and dielectric loss tanδ as a function of Nb_2O_5 content.

The electric-field-induced unipolar strain curves of Nb_2O_5-modified 0.8PHT-0.2PMN are shown in Fig. 4a. The corresponding effective high-field piezoelectric strain coefficient d^*_{33} and strain hysteresis H were calculated according to previous reports [15, 31] and given in Fig. 4b. It was found that both d^*_{33} and H were improved significantly with the addition of Nb_2O_5, from 560 pm V^{-1} and 10% to 700 pm V^{-1} and 16%, respectively. The donor dopants enter into the lattice structure to substitute B-site ions and generate Pb^{2+} vacancies, favoring the movement of ferroelectric domain walls. Consequently, the higher d^*_{33} values and strain hysteresis for the compositions with higher Nb_2O_5 content mainly attributes to the higher extrinsic contribution (domain wall motion) in ceramics.

The piezoelectric and dielectric properties of Nb_2O_5-modified 0.8PHT-0.2PMN are shown in Fig. 5. The piezoelectric coefficient d_{33} and planar electromechanical coupling k_p were found to increase firstly, reaching the maxima of 670 pC N^{-1} and 71%, respectively, and then decrease significantly with Nb_2O_5 being higher than 0.2 wt%. On the other hand, the dielectric permittivity ε_r decreased slightly with Nb doping, while dielectric loss tanδ increased linearly. In a polycrystalline system, dielectric and piezoelectric properties depend on both intrinsic (lattice deformation) and extrinsic (domain walls and defect dipoles) mechanisms [32–35]. It is clear that a phase transformation from tetragonal to rhombohedral phase was observed as discussed in the XRD patterns (Fig. 1), resulting in the reduced polarizability in Nb-doped compositions (Fig. 3), which will lead to the decrease of dielectric and piezoelectric properties. Meanwhile, the high extrinsic contribution (domain wall motion) induced by Pb^{2+} vacancies improves the dielectric and piezoelectric properties with increased dielectric loss. Consequently, the integrated intrinsic and extrinsic mechanisms induced by Nb doping contributed to the property evolution in the PHT-PMN system.

The detailed dielectric, piezoelectric, and ferroelectric properties for Nb_2O_5-modified 0.8PHT-0.2PMN, compared with commercial soft PZT ceramics, are summarized in Table 1. It was found that, compared to the commercial PZT5H ceramics, the 0.8PHT-0.2PMN ceramics doped with 0–0.5 wt%Nb_2O_5 possess not only improved piezoelectric, electromechanical, and ferroelectric properties, but also much higher Curie temperature, promising for transducer applications.

4 Conclusions In conclusion, Nb_2O_5 doped 0.8PHT-0.2PMN ceramics with compositions near MPB have been fabricated using two-step precursor method. The effects of Nb_2O_5 addition on the phase structure, dielectric, piezoelectric properties, and electric-field-induced polarization and strain of 0.8PHT-0.2PMN were investigated in detail. It was found that Nb doping induced a phase transformation from tetragonal to rhombohedral phase in the PHT-PMN system, leading to the deterioration of polarizability. Furthermore, the electric-field-induced unipolar strain and hysteresis were enhanced significantly, attributed to the improvement of domain wall motion. The optimum piezoelectric and electromechanical properties were achieved for the 0.2 wt% Nb_2O_5-modified 0.8PHT-0.2PMN, with d_{33} of 670 pC N^{-1}, ε_r of 2730, k_p of 71%, tanδ of 1.6%, T_C of 267 °C, P_r of 40.7 $\mu C\,cm^{-2}$, and d^*_{33} of 580 pm V^{-1}, which are promising candidates for transducer applications.

Acknowledgements The authors thank Prof. Thomas R. Shrout for the helpful discussion. The work was supported by the National Natural Science Foundation of China under Grant Nos. 50742007, 50972014, and 51132002, the National High Technology Research and Development Program of China under Grant No. 2007AA03Z103, Beijing Natural Science Foundation under Grant No. 3122013, and Scientific Research Common Program of Beijing Municipal Commission of Education under Grant No. KM201210009004. The author (D. Wang) wishes to acknowledge the support from the China Scholarship Council.

References

[1] B. Jaffe, W. R. Cook, and H. Jaffe, Piezoelectric Ceramics (Academic, New York, 1971).
[2] G. H. Haertling, J. Am. Ceram. Soc. **82**, 797 (1999).
[3] S. J. Zhang et al., Mater. Lett. **59**, 3471 (2005).
[4] H. Ouchi et al., J. Am. Ceram. Soc. **48**, 630 (1965).
[5] K. H. Yoon et al., J. Appl. Phys. **89**, 3915 (2001).
[6] M. Kondo et al., Jpn. J. Appl. Phys. **36**, 6043 (1997).
[7] R. Cao et al., J. Am. Ceram. Soc. **93**, 737 (2010).
[8] H. Hao et al., J. Appl. Phys. **105**, 024104 (2009).
[9] H. Hao et al., J. Am. Ceram. Soc. **91**, 2232 (2008).
[10] K. H. Yoon et al., J. Am. Ceram. Soc. **85**, 2753 (2002).
[11] J. B. Lim et al., Ceram. Int. **38**, 277 (2012).
[12] G. Fantozzi et al., J. Eur. Ceram. Soc. **20**, 1671 (2000).
[13] B. Jaffe et al., J. Res. Natl. Bureau Stand. **55**, 239 (1955).
[14] D. W. Wang et al., Phys. Status Solidi RRL **6**, 135 (2012).
[15] D. W. Wang et al., J. Am. Ceram. Soc. **95**, 3220 (2012).
[16] K. Reichmann et al., J. Mater. Sci. **45**, 1473 (2010).
[17] D. W. Wang et al., Phys. Status Solidi RRL **7**, 221 (2013).
[18] M. S. Cao et al., Mater. Lett. **64**, 1798 (2010).
[19] D. W. Wang et al., Chin. Phys. B **18**, 2596 (2009).
[20] M. Pereira et al., J. Eur. Ceram. Soc. **21**, 1353 (2001).
[21] J. E. Garcia et al., J. Eur. Ceram. Soc. **27**, 4029 (2007).
[22] S. Chen et al., J. Am. Ceram. Soc. **90**, 477 (2007).
[23] O. P. Thakur et al., Mod. Phys. Lett. B **19**, 1783 (2005).
[24] D. W. Wang et al., J. Mater. Sci. **47**, 2687 (2012).
[25] D. W. Wang et al., J. Am. Ceram. Soc. **94**, 647 (2011).
[26] S. J. Yoon et al., J. Am. Ceram. Soc. **80**, 1035 (1997).
[27] IEEE Standard on Piezoelectricity, ANSI/IEEE Std 176-1987 (American Standards National Institute, New York, 1987).
[28] S. J. Zhang et al., IEEE Trans. Ultrason. Ferroelectr. Freq. Control **52**, 2131 (2005).
[29] Y. Xu, Ferroelectric Materials and Their Applications (Elsevier Science Publishers B.V., The Netherlands, 1991).
[30] C. A. Randall et al., J. Am. Ceram. Soc. **81**, 677 (1998).
[31] S. J. Zhang et al., Solid State Commun. **137**, 16 (2006).
[32] W. Cao et al., J. Phys. Chem. Solids **57**, 1499 (1996).
[33] R. Herbiet et al., Ferroelectrics **98**, 107 (1989).
[34] D. Damjanovic et al., Appl. Phys. Lett. **68**, 3046 (1996).
[35] Q. M. Zhang et al., J. Appl. Phys. **75**, 454 (1994).
[36] D. Berlincount et al., Ultrasonic Transducer Materials (Plenum, New York, London, 1971).